

Noncanonical Spectral Model of Multidimensional Uniform Random Fields

A. B. Borzov^a, L. V. Labunets^{a,*}, and V. B. Steshenko^a

^a*Bauman Moscow State Technical University, Russian Space Systems, Moscow, 105005 Russia*

**e-mail: labunets@bmstu.ru*

Received October 10, 2017; in final form, June 26, 2018

Abstract—The estimates for the power spectrum of multidimensional uniform random fields in the form of models of finite mixtures of standard spectra are proposed. The learning algorithm of the models demonstrates improved convergence properties for degenerate spectra and small interclass distances in the frequency space, as well as for small volumes of the experimental data. Based on this, the noncanonical models of uniform random fields are presented as a sum of statistically independent spatial harmonics with random amplitudes and frequencies. The alternative representation of a multidimensional spectrum as a sample of random frequencies allowed us to propose computationally efficient algorithms of digital synthesis of background and underlying surface images with the topology of spectral estimates that are adequate for the experimental data. The algorithms are free from simplifying assumptions regarding the method of discretization of the field and functional form of the power spectral density.

DOI: 10.1134/S1064230718060047

INTRODUCTION

The functioning of optical-electronic, radar, and hydroacoustic control systems is related to the necessity of analyzing rapid processes, which are characterized by non-Gaussian distributions and nonstationarity on the time interval of decision-making. For example, the specifics of correlation-extreme guidance aircraft systems require taking into account the contribution of backgrounds or underlying surfaces in the received signal. An attempt to describe the power spectrum of the corresponding random fields using the traditional autoregression—moving average model, leads, as a rule, to an inadequate description of the statistical characteristics of the input influences in comparison with the experimental data. A significant property of the analysis of the control system's functioning is the small volume of experimental data. In this situation, the classic nonparametric estimates of the fields' statistics become inefficient.

Developing a theory of digital processing of the target fields and signals in the control systems requires taking into account the above-mentioned constraints. Thus, one of the most complex problems is to create a logically consistent sequence of theoretical and computational methods for the statistical modeling of the input influences in the autonomous information systems of remote sensing.

An adequate statistical description of actual nonstationary non-Gaussian signals and noises in the control systems requires models with random parameters. The values of these parameters represent a sample of their probability mixtures of standard distributions [1–4]. We will call such models randomized. Identifying the parameters of these models requires, in turn, applying the methodology of the adaptation and learning theory, including a powerful method of constructing the parametric models of multidimensional non-Gaussian distributions such as the family of expectation-maximization (EM) algorithms [4].

The specifics of the functioning of remote sensing systems is associated with the necessity of locating a target against the background of the underlying surface. A large number of studies is dedicated to the problem of the statistical modeling of backgrounds and underlying surfaces with a specified or experimentally measured power spectral density (PSD) $P(\mathbf{U})$, where $\mathbf{U} = (u_1, \dots, u_N)^T$ is the column vector of the arguments in the frequency domain. However, there is still no final solution to the problems of digital synthesis of multidimensional random fields based on constructing the effective statistical models and algorithms that are free from the a priori simplifying assumptions regarding the functional form of the power spectrum, the method of the field's discretization, its type, and the large volume of experimental data.

One of the possible solutions of this important problem is based on the use of randomized spectral models and presented in this study.

1. STATEMENT OF THE PROBLEM

In comparison with the algorithmic models, the analytical models of random fields [2, 3] have a number of advantages. They provide a match between the covariation function and one-dimensional probability density of the model and the actual influence for uniform random fields of a general form. Being the determined functions of random arguments (parameters), the analytical (parametric) models are more universal in the sense that they can be used in both the digital and analytical analysis of the functioning of control systems.

The parametric models based on the spectral expansion method by Karhunen–Loève–Pugachev have become widespread [5]. Their use is appropriate when the dimensionality of the random field does not exceed two, and the observational interval is not more than 10 correlation radii of the field. The models of one-dimensional input influences based on the spectral expansion method by Chernetskii are characterized by simplicity and cost effectiveness [3]. The development of spectral expansions of uniform multidimensional random fields is the subject of a number of studies by Shalygin and Palagin [2]: they propose modeling algorithms for a series of generic monotonic covariation functions. The question of modeling non-Gaussian fields has not been comprehensively addressed. However, the fields with oscillating covariation functions and nonnormal one-dimensional distributions are quite often encountered in practice [6–10].

We will represent the noncanonical spectral model of the initial N -dimensional Gaussian random field $z(\mathbf{X})$ as a sum of statistically independent spatial harmonics $y_m(\mathbf{X})$ with random amplitudes a_m and frequencies Ω_m [1, 2, 11]:

$$z(\mathbf{X}) = \frac{1}{\sqrt{M}} \sum_{m=1}^M y_m(\mathbf{X}); \quad y_m(\mathbf{X}) = \sqrt{2}a_m \sin\{\Omega_m^T(\mathbf{X} + \mathbf{X}_0) + \pi/4\}. \quad (1.1)$$

Here, $\mathbf{X} = (x_1, \dots, x_N)^T$ is the column vector of the arguments in the spatial domain; $\mathbf{X}_0 = (x_{01}, \dots, x_{0N})^T$ is the vector of the initial displacement [2]; and $\Omega_1, \dots, \Omega_M$ and a_1, \dots, a_M are mutually independent samples of random spatial frequencies and amplitudes.

It is important to note that a *sample of random frequencies* is an effective alternative (in terms of computational costs) to a multidimensional regular discretization grid in the frequency domain. In other words, in the context of noncanonical spectral models, the normalized PSD $P(\mathbf{U})$ acquires the sense of a multidimensional probability density function $P(\Omega)$ of the *random frequency* vector $\Omega = (\omega_1, \dots, \omega_N)^T$ [1, 2].

Thus, in accordance with model (1.1), the digital synthesis of a Gaussian random field with null mathematical expectation and unit variance at the first stage is reduced to the generation of amplitudes a_m . The reversal method for a random value a with a symmetric Rayleigh distribution $|a| \exp(-a^2)$, $a \in (-\infty, +\infty)$ yields the following modeling algorithm [12]: $a_m = \chi(-\ln\gamma)$, where χ and γ are independent; γ is uniformly distributed in the interval [0, 1]; and χ takes values ± 1 with equal probability.

At the second stage, in accordance with the probability density function $P(\Omega)$, random frequencies Ω_m are generated. The field value at the final stage is calculated by formula (1.1) in any given point of the initial space. Choosing the initial displacement vector \mathbf{X}_0 equal to three or five correlation intervals of the modeled field ensures the uniformity and normality of its one-dimensional distribution at the number of harmonics $M \geq 5 \dots 10$ [2].

2. RANDOMIZED SPECTRAL ANISOTROPIC MODEL

The standard spectral estimates are formed on a regular raster of the frequency space (Fig. 1a). However, for the fields with a dimensionality of at least two, it is more computationally effective to use the alternative form of representation of the power spectrum as a scatter diagram (Fig. 1b). The coordinate axes u_1 and u_2 of the two-dimensional grid of spatial frequencies in Fig. 1 have a dimensionality of m^{-1} . It is reasonable to represent the sample of random frequencies in the spectral model (1.1) as points in the corresponding frequency space, which are classified into a finite number of statistically uniform clusters. Such an interpretation is productive in the modeling of uniform *anisotropic* fields, since it substantiates

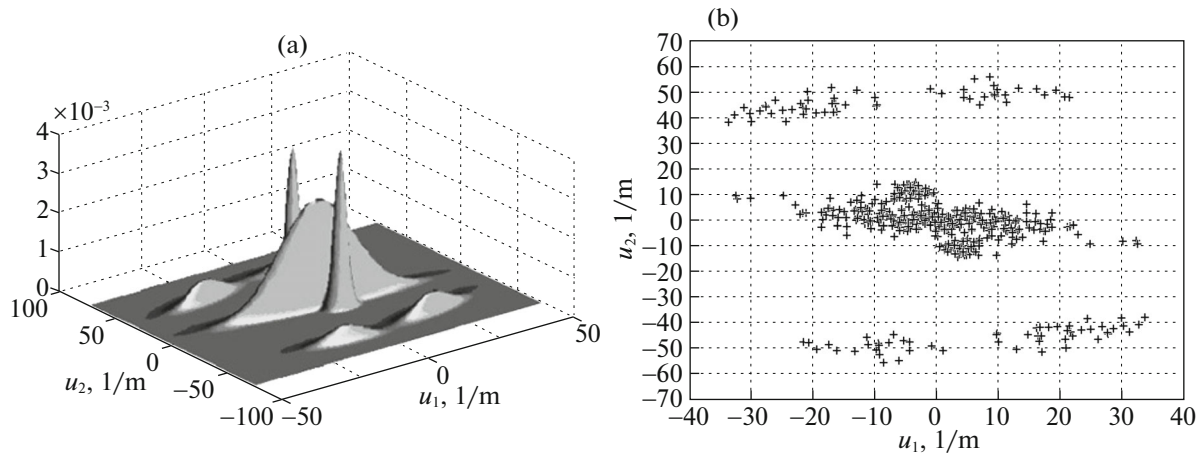


Fig. 1. Alternative representations of power spectrum of image: (a) regular raster; (b) sample of random frequencies.

the approximation of the power spectrum of the field with a finite mixture of generic multidimensional spectral densities. In this approach, the computationally effective algorithms for the identification of the mixture parameters are based on the methods of the adaptation and learning theory.

A series of models of random fields with elliptical and multiplicative anisotropy are presented in [2]. However, such simplest kinds of anisotropy inadequately model the correlational structure of the majority of actual influences of control systems [7–10]. Let us consider the procedure for immersing the spectral model of a uniform anisotropic Gaussian random field into the space of frequency attributes.

In the parametric representation of a random field (1.1), it is rational to interpret the sample of random frequencies $\Omega_1, \dots, \Omega_M$ as a set of points in the N -dimensional space of images $\{u_1, \dots, u_N\}$, i.e., represent it as an N -dimensional scatter diagram. In this case, the anisotropy of the modeled field will be expressed in the fact that the whole set of points is classified into a finite number of pairs of centrally symmetric uniform subsets (classes) that are grouped in the frequency space $\{u_1, \dots, u_N\}$ in certain ranges of directions or compact nonintersecting regions [7, p. 89; 9, p. 42].

It is rational to represent each uniform pair of centrally symmetric groups of points as a general population, which is specified with its probability density as a two-component mixture of standard distributions $S_k(\mathbf{U}, \theta_k) = \{s_k(\mathbf{U} - \mathbf{A}_k, B_k) + s_k(\mathbf{U} + \mathbf{A}_k, B_k)\}/2$. The parameters $\theta_k = (\mathbf{A}_k, B_k)$ specify the position (with the mathematical expectation vector \mathbf{A}_k) and scale (with the covariation matrix B_k) of the k th centrally symmetric partial distribution. In other words, the power spectrum $P(\mathbf{U})$ of the anisotropic field is convenient to approximate with a finite mixture of generic multidimensional spectral densities

$$S(\mathbf{U}, \theta) = \sum_{k=1}^K p_k S_k(\mathbf{U}, \theta_k), \quad \sum_{k=1}^K p_k = 1, \quad (2.1)$$

which are specified with an accuracy to the final number of their parameters $\theta = (p_1, \dots, p_K, \mathbf{A}_1, \dots, \mathbf{A}_K, B_1, \dots, B_K)$. Here, p_k is the weight of the k th anisotropic component of the field.

The advantage of representation (2.1) is obvious, since the digital modeling of the random frequency vector Ω in this case is performed with the effective method of the superposition of the algorithms for modeling standard random values [2, 12].

3. SPECTRAL MODELS IN THE MAHALANOBIS METRICS

A rather wide class of the random field power spectrum can be approximated with multidimensional distributions in the Mahalanobis metrics $D^2(\mathbf{U} - \mathbf{A}_k, B_k) = (\mathbf{U} - \mathbf{A}_k)^T B_k^{-1} (\mathbf{U} - \mathbf{A}_k)$ [1, 4, 13]. Within such models, generic spectral densities $S_k(\mathbf{U}, \theta_k)$ of anisotropic components are represented as N -dimensional ellipsoidally symmetric distributions with different mathematical expectation vectors \mathbf{A}_k and covariation matrices B_k [13]:

$$S_k(\mathbf{U}, \boldsymbol{\theta}_k) = \frac{f\{D^2(\mathbf{U} - \mathbf{A}_k, B_k)\} + f\{D^2(\mathbf{U} + \mathbf{A}_k, B_k)\}}{2S_1 v_{N-1} \sqrt{|\det B_k|}},$$

$$v_{N-1} = \int_0^\infty r^{N-1} f(r^2) dr. \quad (3.1)$$

Here, $D^2(\mathbf{U} + \mathbf{A}_k, B_k) = (\mathbf{U} + \mathbf{A}_k)^T B_k^{-1} (\mathbf{U} + \mathbf{A}_k)$ is the Mahalanobis metrics of the spectral subclass with the center of the frequency group at the point with a radius vector $(-\mathbf{A}_k)$; $S_1 = 2\sqrt{\pi^N} \Gamma^{-1}(N/2)$ is the surface area of a unit hypersphere in the N -dimensional frequency space; and $S_1^{-1} v_{N-1}^{-1} f(r^2)$ is a monotonically decreasing (as $r \rightarrow \infty$) radial distribution with a finite $(N-1)$ th central moment v_{N-1} . Three types of radial basis functions became widespread in practice [4, 14, 15].

The Gauss function:

$$f(r^2) = \exp\left(-\frac{r^2}{2}\right), \quad v_{N-1} = \frac{1}{2} \sqrt{2^N} \Gamma\left(\frac{N}{2}\right);$$

the Pierson function with the parameter $\gamma \geq 0$:

$$f(r^2) = \begin{cases} \left(1 - \frac{r^2}{2\gamma + N}\right)^{\gamma-1}, & r^2 \leq 2\gamma + N, \\ 0, & r^2 > 2\gamma + N, \end{cases}$$

$$v_{N-1} = \frac{1}{2} \sqrt{(2\gamma + N)^N} B\left(\gamma, \frac{N}{2}\right);$$

the Student function with the parameter $\gamma > N-1$:

$$f(r^2) = \left(1 + \frac{r^2}{\gamma + 1 - N}\right)^{-\frac{\gamma+1}{2}},$$

$$v_{N-1} = \frac{1}{2} \sqrt{(\gamma + 1 - N)^N} B\left(\frac{\gamma + 1 - N}{2}, \frac{N}{2}\right),$$

where $B(\eta, \mu) = \Gamma(\eta)\Gamma(\mu)\Gamma^{-1}(\eta + \mu)$ is the beta function and $\Gamma(\eta)$ is the gamma function.

4. LEARNING THE SPECTRAL MODEL

It is rational to identify the parameters of the spectral model (2.1) using an indirect method. Such an approach involves a preliminary stage of selective estimation of the power spectrum $P(\mathbf{U})$ by the experimentally measured "image" of a multidimensional random field. The Fourier analysis of the data with a high frequency resolution and sufficiently low variance of the estimate is based on the use of the methods of the linear prediction theory [16]. In particular, the autoregression spectral estimation of relatively small units of data using a modified covariation method [17, 18] makes it possible to obtain reliable spectral estimates and verify the adequacy of the modeled random field relative to the experimental measurements.

The effective realization of the step of identifying the parameters of model (2.1) is based on the use of the Stochastic Weighing Maximization (SWM) algorithm [19]. The standard learning goal, in this case, is the maximization of the Fisher likelihood functional:

$$\boldsymbol{\theta}_{\text{opt}} = \arg \max_{\boldsymbol{\theta}} \{L(\boldsymbol{\theta})\}, \quad L(\boldsymbol{\theta}) = \int_{R^N} P(\mathbf{U}) \ln\{S(\mathbf{U}, \boldsymbol{\theta})\} d\mathbf{U}.$$

The rational learning goal is the minimization of the Bhattacharya distance functional [19]:

$$\boldsymbol{\theta}_{\text{opt}} = \arg \min_{\boldsymbol{\theta}} \{d(\boldsymbol{\theta})\}, \quad d(\boldsymbol{\theta}) = -\ln \int_{R^N} \sqrt{P(\mathbf{U})S(\mathbf{U}, \boldsymbol{\theta})} d\mathbf{U}.$$

Solving these problems of conditional optimization using the method of indeterminate Lagrange multipliers yields a system of nonlinear equations [19] with respect to the parameters θ of partial spectra. The canonical form of this system that allows its solution by the method of successive approximations appears as follows:

$$\begin{cases} p_k = \frac{w_k(\theta)}{\sum_{j=1}^K w_j(\theta)}, \\ \mathbf{A}_k = \frac{\lambda_k(\theta)}{v_k(\theta)}, \\ B_k = -\frac{2\{c_k(\theta) - v_k(\theta)\mathbf{A}_k\mathbf{A}_k^T\}}{w_k(\theta)}, \end{cases} \quad (4.1)$$

where

$$\begin{aligned} w_k(\theta) &= \int_{R^N} w(\mathbf{U}, \theta) Sr(k|\mathbf{U}, \theta) d\mathbf{U}, \quad k = \overline{1, K}; \\ v_k(\theta) &= \int_{R^N} w(\mathbf{U}, \theta) \{F(\mathbf{U} - \mathbf{A}_k, B_k) + F(\mathbf{U} + \mathbf{A}_k, B_k)\} Sr(k|\mathbf{U}, \theta) d\mathbf{U}; \\ \lambda_k(\theta) &= \int_{R^N} \mathbf{U} w(\mathbf{U}, \theta) \{F(\mathbf{U} - \mathbf{A}_k, B_k) - F(\mathbf{U} + \mathbf{A}_k, B_k)\} Sr(k|\mathbf{U}, \theta) d\mathbf{U}; \\ c_k(\theta) &= \int_{R^N} \mathbf{U}\mathbf{U}^T w(\mathbf{U}, \theta) \{F(\mathbf{U} - \mathbf{A}_k, B_k) + F(\mathbf{U} + \mathbf{A}_k, B_k)\} Sr(k|\mathbf{U}, \theta) d\mathbf{U}. \end{aligned}$$

Here, $Sr(k|\mathbf{U}, \theta) = p_k S_k(\mathbf{U}, \theta_k) / S(\mathbf{U}, \theta)$ is the a posteriori spectrum (which acquires the sense of the a posteriori probability density function within the randomized model) with parameters θ , which characterizes the extent to which the spatial frequency vector \mathbf{U} belongs to the k th spectral class. The vertical line in this expression indicates the conditional character of the distribution similar to the notations adopted in the Bayes models. The a posteriori spectra satisfy the following obvious properties:

$$Sr(k|\mathbf{U}, \theta) \geq 0, \quad \sum_{k=1}^K Sr(k|\mathbf{U}, \theta) = 1.$$

The weight function $w(\mathbf{U}, \theta)$ is determined by the functional of the quality of the mixture's parameter estimates:

$$w(\mathbf{U}, \theta) = \begin{cases} P(\mathbf{U}) & \text{for likelihood,} \\ \sqrt{P(\mathbf{U})S(\mathbf{U}, \theta)} & \text{for distance.} \end{cases}$$

The modifiers

$$F(\mathbf{U} \mp \mathbf{A}_k, B_k) = \frac{\partial f\{D^2(\mathbf{U} \mp \mathbf{A}_k, B_k)\} / \partial D^2}{f\{D^2(\mathbf{U} - \mathbf{A}_k, B_k)\} + f\{D^2(\mathbf{U} + \mathbf{A}_k, B_k)\}}$$

depend on the choice of the type of radial distributions in the finite mixture model (2.1).

The multidimensional integrals in the equation system (4.1) have a distinct statistical sense. In particular, it is appropriate to interpret $w_k(\theta)$ and $v_k(\theta)$ as the a posteriori dispersion and modified dispersion of the k th spectral class. Correspondingly, $\lambda_k(\theta)$ and $c_k(\theta)$ acquire the sense of the a posteriori characteristics of the position (mathematical expectation vector) and scale (covariation matrix) of the k th spectral class.

In a two-dimensional ($N = 2$) frequency space, the estimates of the above mentioned integrals do not require significant computational resources, since they can be acquired based on the standard cubature algorithms. Figure 2 shows the poly-Gaussian approximation $S(\mathbf{U}, \theta)$ of the power spectrum $P(\mathbf{U})$ of the radar image obtained as a result of remotely sensing the rough sea surface with a side-looking radar [7].

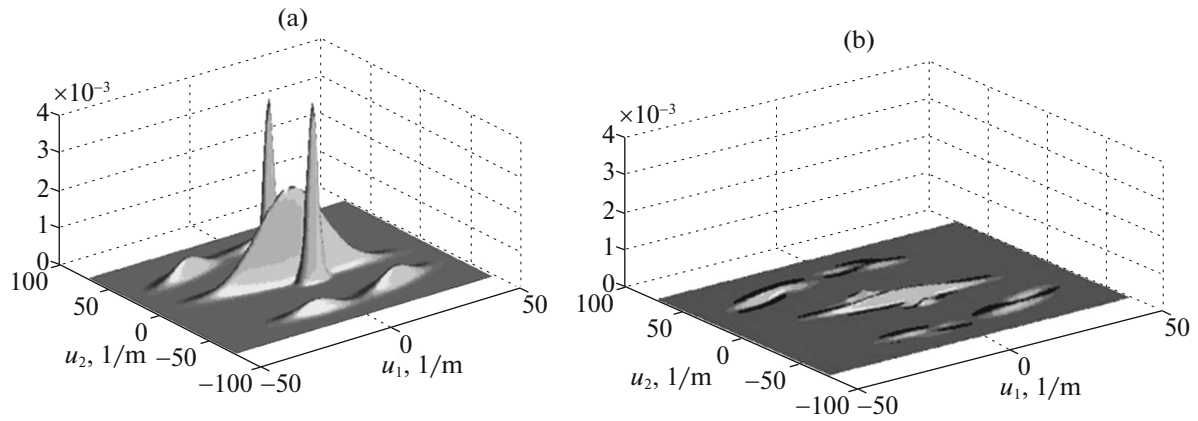


Fig. 2. Poly-Gaussian approximation of power spectrum of radar sea image: (a) model; (b) model error.

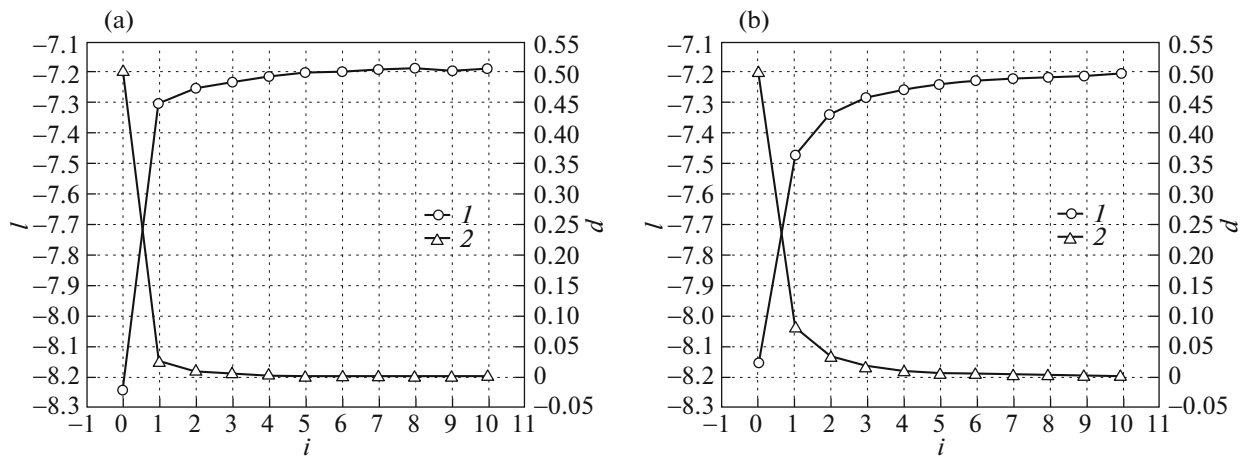


Fig. 3. Convergence of SWM learning algorithm for model: (a) by likelihood criterion; (b) by distance criterion.

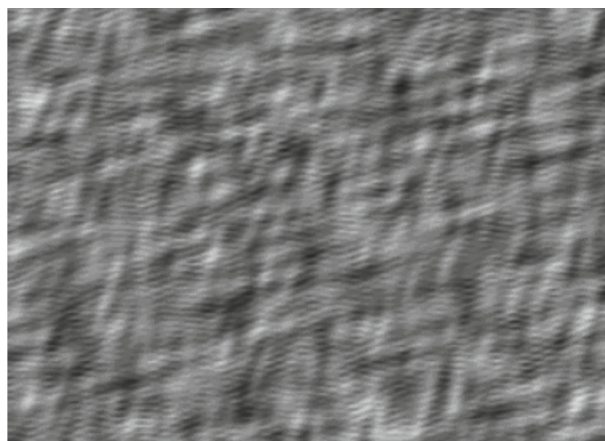


Fig. 4. Model image of rough sea surface.

The convergence of the SWM algorithm by the iterations $i = 1, 2, \dots$ of successive approximations of the search for the optimal mixture parameters (2.1) of the Gaussian partial spectra is illustrated in Fig. 3. Curves 1 and 2 demonstrate the variations in the likelihood and distance functionals on the scales of the left and right vertical axes, respectively. The results of the digital modeling of an image of the sea using the spectral model (1.1) with 500 spatial harmonics are shown in Fig. 4.

5. SWM LEARNING ALGORITHM OF THE SPECTRAL MODEL

In the frequency space with a dimensionality above two ($N > 2$), the efficient computational algorithm for estimating the multidimensional integrals in the equation system (4.1) is based on the use of the essential sample method [12]. As shown in [19], for this purpose general it is rational to choose populations of random values that are characterized by the distributions $S_k(\mathbf{U}, \boldsymbol{\theta}_k)$, $k = \overline{1, K}$. This method is implemented by choosing a modified weight function:

$$W(\mathbf{U}, \boldsymbol{\theta}) = \frac{w(\mathbf{U}, \boldsymbol{\theta})}{S(\mathbf{U}, \boldsymbol{\theta})} = \begin{cases} \frac{P(\mathbf{U})}{S(\mathbf{U}, \boldsymbol{\theta})} & \text{for likelihood,} \\ \sqrt{\frac{P(\mathbf{U})}{S(\mathbf{U}, \boldsymbol{\theta})}} & \text{for distance.} \end{cases}$$

The substitution of $w(\mathbf{U}, \boldsymbol{\theta}) = W(\mathbf{U}, \boldsymbol{\theta})S(\mathbf{U}, \boldsymbol{\theta})$ into the expressions for the integrals of system (4.1) gives the modified equation system by the iterations $i = 1, 2, \dots$ of successive approximations:

$$\begin{cases} p_k [i] = \frac{p_k [i - 1] W_k(\boldsymbol{\theta} [i - 1])}{\sum_{j=1}^K p_j [i - 1] W_j(\boldsymbol{\theta} [i - 1])}, \\ \mathbf{A}_k [i] = \frac{\boldsymbol{\Lambda}_k(\boldsymbol{\theta} [i - 1])}{V_k(\boldsymbol{\theta} [i - 1])}, \\ B_k [i] = -\frac{2G\{C_k(\boldsymbol{\theta} [i - 1]) - V_k(\boldsymbol{\theta} [i - 1])\mathbf{A}_k [i - 1]\mathbf{A}_k^T [i - 1]\}}{W_k(\boldsymbol{\theta} [i - 1])}. \end{cases} \tag{5.1}$$

Considering the equations

$$F(\mathbf{U} \mp \mathbf{A}_k, B_k) S_k(\mathbf{U}, \boldsymbol{\theta}_k) = \frac{S_k^\pm(\mathbf{U}, \boldsymbol{\theta}_k)}{2},$$

$$S_k^\pm(\mathbf{U}, \boldsymbol{\theta}_k) = \frac{\partial f\{D^2(\mathbf{U} \mp \mathbf{A}_k, B_k)\} / \partial D^2}{S_1 V_{N-1} \sqrt{|\det B_k|}},$$

the multidimensional integrals in system (5.1) acquire a form that is convenient for estimation by the Monte Carlo Method:

$$W_k(\boldsymbol{\theta}) = \int_{R^N} W(\mathbf{U}, \boldsymbol{\theta}) S_k(\mathbf{U}, \boldsymbol{\theta}_k) d\mathbf{U};$$

$$V_k(\boldsymbol{\theta}) = \int_{R^N} W(\mathbf{U}, \boldsymbol{\theta}) g_k(\mathbf{U}, \boldsymbol{\theta}_k) d\mathbf{U};$$

$$\boldsymbol{\Lambda}_k^\pm(\boldsymbol{\theta}) = \int_{R^N} \mathbf{U} W(\mathbf{U}, \boldsymbol{\theta}) g_k^\pm(\mathbf{U}, \boldsymbol{\theta}_k) d\mathbf{U};$$

$$\boldsymbol{\Lambda}_k(\boldsymbol{\theta}) = \frac{1}{2} \{\boldsymbol{\Lambda}_k^+(\boldsymbol{\theta}) - \boldsymbol{\Lambda}_k^-(\boldsymbol{\theta})\};$$

$$C_k(\boldsymbol{\theta}) = \int_{R^N} \mathbf{U} \mathbf{U}^T W(\mathbf{U}, \boldsymbol{\theta}) g_k(\mathbf{U}, \boldsymbol{\theta}_k) d\mathbf{U}, \quad k = \overline{1, K}.$$

Here, $g_k(\mathbf{U}, \boldsymbol{\theta}_k) = \{g_k^+(\mathbf{U}, \boldsymbol{\theta}_k) + g_k^-(\mathbf{U}, \boldsymbol{\theta}_k)\} / 2$ is the two-component mixture of standard distributions

$$g_k^\pm(\mathbf{U}, \boldsymbol{\theta}_k) = \frac{1}{G} S_k^\pm(\mathbf{U}, \boldsymbol{\theta}_k), \tag{5.2}$$

where

$$G = \frac{\int_{R^N} \frac{\partial f\{D^2(\mathbf{U} - \mathbf{z}, B_k)\}}{\partial D^2} d\mathbf{U}}{S_1 v_{N-1} \sqrt{|\det B_k|}} = \frac{\int_{R^N} \frac{\partial f(r^2)}{\partial r^2} d\mathbf{u}}{S_1 v_{N-1}} = \frac{\int_0^\infty r^{N-1} \frac{\partial f(r^2)}{\partial r^2} dr}{v_{N-1}} \tag{5.3}$$

is the normalizing multiplier; $\mathbf{z} = (0, 0, \dots, 0)^T$ is the N -dimensional null column-vector; $r = \|\mathbf{u}\|$ is the Euclidian distance in the space of the normalized frequencies $\mathbf{u} = \delta_k^{-1} \omega_k^T \mathbf{U}$ obtained with a decorrelating transform [20]; and δ_k and ω_k are the matrices of singular numbers and eigenvectors of the covariation matrix B_k of the spectral class.

The expressions for the integrals from the derivatives of the basis functions in formula (5.3) can be found in the reference book [21]. The subsequent transforms in accordance with Eqs. (5.2) allow us to obtain a family of N -dimensional ellipsoidally symmetric distributions.

Gauss distribution:

$$g_k^\pm(\mathbf{U}, \boldsymbol{\theta}_k) = \frac{\exp\{-D^2(\mathbf{U} \mp \mathbf{A}_k, B_k)/2\}}{\sqrt{(2\pi)^N |\det B_k|}},$$

$$g_k(\mathbf{U}, \boldsymbol{\theta}_k) = S_k(\mathbf{U}, \boldsymbol{\theta}_k); \quad G = -1/2;$$

Pierson distribution:

$$g_k^\pm(\mathbf{U}, \boldsymbol{\theta}_k) = \begin{cases} \rho_k \left[1 - \frac{D^2(\mathbf{U} \mp \mathbf{A}_k, B_k)}{(2\gamma - 2 + N)\sigma^2} \right]^{\gamma-2}, & D^2(\mathbf{U} \mp \mathbf{A}_k, B_k) \leq 2\gamma + N, \\ 0, & D^2(\mathbf{U} \mp \mathbf{A}_k, B_k) > 2\gamma + N, \end{cases}$$

$$\rho_k = \frac{\Gamma\left(\gamma - 1 + \frac{N}{2}\right)}{\Gamma(\gamma - 1) \sigma^N \sqrt{\{\pi(2\gamma - 2 + N)\}^N |\det B_k|}};$$

$$G = -1/(2\sigma^2);$$

Student distribution:

$$g_k^\pm(\mathbf{U}, \boldsymbol{\theta}_k) = \rho_k \left\{ 1 + \frac{D^2(\mathbf{U} \mp \mathbf{A}_k, B_k)}{(\gamma + 3 - N)\sigma^2} \right\}^{-\frac{\gamma+3}{2}},$$

$$\rho_k = \frac{\Gamma\left(\frac{\gamma+3}{2}\right)}{\Gamma\left(\frac{\gamma+3-N}{2}\right) \sigma^N \sqrt{\{\pi(\gamma+3-N)\}^N |\det B_k|}}.$$

$$G = -1/2.$$

It can be easily seen that the partial spectra $g_k^\pm(\mathbf{U}, \boldsymbol{\theta}_k)$ are obtained by the correlating transform $\mathbf{U} = \omega_k \delta_k \mathbf{u} \pm \mathbf{A}_k$ of the family of radial distributions by Gauss $N(\|\mathbf{u}\|, \mathbf{z}, \delta_k^2)$; Pierson $R_{N, \gamma-1}(\|\mathbf{u}\|, \mathbf{z}, \sigma^2 I_N)$ [4, p. 538] with the parameters $\gamma - 1 > 0$ and $\sigma = \sqrt{(2\gamma + N)/(2\gamma - 2 + N)}$; or Student $t_{N, \gamma+2}(\|\mathbf{u}\|, \mathbf{z}, \sigma^2 I_N)$ [4, p. 540] with the parameters $\gamma + 2 > N - 1$ and $\sigma = \sqrt{(\gamma + 1 - N)/(\gamma + 3 - N)}$.

It is important to note that the statistics $\mathbf{A}_k(\boldsymbol{\theta})$ and $C_k(\boldsymbol{\theta})$ are in agreement with the w -weighted (in the sense of L.D. Meshalkin [22]) characteristics of the position and scale of the k th modified partial spectrum.

The quality functionals of the randomized model (2.1) of the field power spectrum are convenient to calculate by the following formulas [19]:

$$L(\boldsymbol{\theta}) = \sum_{k=1}^K p_k L_k(\boldsymbol{\theta}); \quad d(\boldsymbol{\theta}) = -\ln \sum_{k=1}^K p_k d_k(\boldsymbol{\theta}).$$

Here, the w -weighted estimates of likelihood

$$L_k(\boldsymbol{\theta}) = \int_{R^N} W(\mathbf{U}, \boldsymbol{\theta}) \ln\{S(\mathbf{U}, \boldsymbol{\theta})\} S_k(\mathbf{U}, \boldsymbol{\theta}_k) d\mathbf{U}$$

and distance

$$d_k(\boldsymbol{\theta}) = \int_{R^N} W(\mathbf{U}, \boldsymbol{\theta}) S_k(\mathbf{U}, \boldsymbol{\theta}_k) d\mathbf{U}$$

of the k th spectral class are also obtained by the method of the essential sample from the distribution $S_k(\mathbf{U}, \boldsymbol{\theta}_k)$.

The parameters of the spectral model (2.1) are identified using the SWM unsupervised learning algorithm presented in [19]. The algorithm presets the initial approximations of the vector $\boldsymbol{\theta}[0]$ of the parameters that correspond to the initial values of the quality functionals of the spectral density $S(\mathbf{U}, \boldsymbol{\theta}[0])$:

$$\hat{L}_k(\boldsymbol{\theta}[0]) = \frac{1}{M} \sum_{m=1}^M W(\boldsymbol{\Omega}_m^{(k)}[0] + \boldsymbol{\alpha}_m^{(k)}[0], \boldsymbol{\theta}[0]) \ln\{S(\boldsymbol{\Omega}_m^{(k)}[0] + \boldsymbol{\alpha}_m^{(k)}[0], \boldsymbol{\theta}[0])\},$$

$$\hat{d}_k(\boldsymbol{\theta}[0]) = \frac{1}{M} \sum_{m=1}^M W(\boldsymbol{\Omega}_m^{(k)}[0] + \boldsymbol{\alpha}_m^{(k)}[0], \boldsymbol{\theta}[0]).$$

At the S -step of the i th iteration of the algorithm ($i = 1, 2, \dots$), the statistical modeling of the learning samples is performed:

$$\{\boldsymbol{\Omega}_m^{(k)}[i-1] + \boldsymbol{\alpha}_m^{(k)}[i-1]\}, \quad \{\boldsymbol{\Psi}_m^{(k)}[i-1] + \boldsymbol{\alpha}_m^{(k)}[i-1]\}$$

and

$$\{\boldsymbol{\Psi}_m^{(k)}[i-1] \pm \mathbf{A}_k[i-1]\}, \quad m = \overline{1, M}.$$

These samples are the realizations (independent in the population) of the standard random vectors with distributions $S_k(\mathbf{U}, \boldsymbol{\theta}_k)$, $g_k(\mathbf{U}, \boldsymbol{\theta}_k)$, and $g_k^\pm(\mathbf{U}, \boldsymbol{\theta}_k)$. Here, $\boldsymbol{\alpha}^{(k)}$ is the vector that takes the values $\pm \mathbf{A}_k$ with equal probability; $\boldsymbol{\Omega}^{(k)}$ and $\boldsymbol{\Psi}^{(k)}$ are the random frequency vectors, which correspond to the ellipsoidally symmetric distributions

$$\frac{f\{D^2(\mathbf{U} - \mathbf{z}, B_k)\}}{S_1 \nu_{N-1} \sqrt{\det B_k}}, \tag{5.4}$$

and

$$\frac{\partial f\{D^2(\mathbf{U} - \mathbf{z}, B_k)\} / \partial D^2}{GS_1 \nu_{N-1} \sqrt{\det B_k}}, \tag{5.5}$$

respectively.

As shown above, the effective algorithm for the statistical modeling of the random frequency vector $\boldsymbol{\Omega}^{(k)}$ realizes the correlating transform $\boldsymbol{\Omega}^{(k)} = \omega_k \delta_k \boldsymbol{\theta}^{(1)}$ [20, 23] of the standard random sample $\{\boldsymbol{\theta}_m^{(1)}\}$, $m = \overline{1, M}$, characterized by the N -dimensional radial distribution by Gauss $N(\|\mathbf{u}\|, \mathbf{z}, \delta_k^2)$, Pierson $R_{N,\gamma}(\|\mathbf{u}\|, \mathbf{z}, I_N)$ or Student $t_{N,\gamma}(\|\mathbf{u}\|, \mathbf{z}, I_N)$, depending on the chosen basis function $f(\|\mathbf{u}\|^2)$ of distribution (5.4).

It is also obvious that modeling the standard random vector $\boldsymbol{\Psi}^{(k)}$ requires the same algorithm as modeling the vector $\boldsymbol{\Omega}^{(k)}$, namely, $\boldsymbol{\Psi}^{(k)} = \omega_k \delta_k \boldsymbol{\theta}^{(2)}$. The only difference is that the standard random sample $\{\boldsymbol{\theta}_m^{(2)}\}$,

$m = \overline{1, M}$ is characterized by the N -dimensional radial distribution by Pierson $R_{N,\gamma-1}(\|\mathbf{u}\|, \mathbf{z}, \sigma^2 I_N)$ or Student $t_{N,\gamma+2}(\|\mathbf{u}\|, \mathbf{z}, \sigma^2 I_N)$ for the corresponding basis function of the modified distribution (5.5).

It is important to note that the S-step of the SWM procedure for the power spectrum's randomization naturally provides the sample of the random frequency vector:

$$\boldsymbol{\Omega}_m = \sum_{k=1}^K \varepsilon_m^{(k)} \{\boldsymbol{\Omega}^{(k)} + \boldsymbol{\alpha}_m^{(k)}\}, \quad m = \overline{1, M},$$

which is necessary for modeling the random field using spectral model (1.1). Here, $\mathbf{E} = (\varepsilon^{(1)}, \dots, \varepsilon^{(K)})^T$ is the random vector that follows the polynomial distribution with the parameters M and $\mathbf{p} = (p_1, \dots, p_K)^T$ [14]; i.e., $\varepsilon^{(k)}$ are the discrete random values that equal 0 or 1 with probabilities $(1 - p_k)$ and p_k , so that $\varepsilon^{(1)} + \dots + \varepsilon^{(K)} = M$.

At the W-step of the i th iteration of the SWM procedure for the power spectrum randomization, the average weights and w -weighted characteristics of the position and scale of the partial spectra are estimated using the essential sample method:

$$\begin{aligned} W_k(\boldsymbol{\theta}[i-1]) &= \frac{1}{M} \sum_{m=1}^M W(\boldsymbol{\Omega}_m^{(k)} + \boldsymbol{\alpha}_m^{(k)}, \boldsymbol{\theta}[i-1]); \\ V_k(\boldsymbol{\theta}[i-1]) &= \frac{1}{M} \sum_{m=1}^M W(\boldsymbol{\Psi}_m^{(k)} + \boldsymbol{\alpha}_m^{(k)}, \boldsymbol{\theta}[i-1]); \\ \Lambda_k^{\pm}(\boldsymbol{\theta}[i-1]) &= \frac{1}{M} \sum_{m=1}^M (\boldsymbol{\Psi}_m^{(k)} \pm \mathbf{A}_k[i-1]) W(\boldsymbol{\Psi}_m^{(k)} \pm \mathbf{A}_k[i-1], \boldsymbol{\theta}[i-1]); \\ \Lambda_k(\boldsymbol{\theta}[i-1]) &= \frac{1}{2} \{\Lambda_k^+(\boldsymbol{\theta}[i-1]) - \Lambda_k^-(\boldsymbol{\theta}[i-1])\}, \quad k = 1, 2, \dots, K; \\ C_k(\boldsymbol{\theta}[i-1]) &= \frac{1}{M} \sum_{m=1}^M (\boldsymbol{\Psi}_m^{(k)} + \boldsymbol{\alpha}_m^{(k)}) (\boldsymbol{\Psi}_m^{(k)} + \boldsymbol{\alpha}_m^{(k)})^T W(\boldsymbol{\Psi}_m^{(k)} + \boldsymbol{\alpha}_m^{(k)}, \boldsymbol{\theta}[i-1]). \end{aligned} \quad (5.6)$$

It is important to underline that, unlike the selective EM algorithm [24], the weight function $W(\mathbf{U}, \boldsymbol{\theta})$ is practically independent of the interclass distances. Thus, an acceptable convergence rate of the SWM algorithm for the randomization of mixture (2.1) should be expected in the case when the partial spectra in the Mahalanobis metrics significantly overlap.

The M-step of the power spectrum's randomization procedure realizes the i th iteration of the search for the solution of modified equation system (5.1) of the successive approximation method. The corresponding current estimates of the quality functionals for the vector $\boldsymbol{\theta}[i]$ of the partial spectra parameters are calculated by the formulas

$$\begin{aligned} \hat{L}_k(\boldsymbol{\theta}[i]) &= \frac{1}{M} \sum_{m=1}^M W(\boldsymbol{\Omega}_m^{(k)}[i] + \boldsymbol{\alpha}_m^{(k)}[i], \boldsymbol{\theta}[i]) \ln \{S(\boldsymbol{\Omega}_m^{(k)}[i] + \boldsymbol{\alpha}_m^{(k)}[i], \boldsymbol{\theta}[i])\}, \\ \hat{d}_k(\boldsymbol{\theta}[i]) &= \frac{1}{M} \sum_{m=1}^M W(\boldsymbol{\Omega}_m^{(k)} + \boldsymbol{\alpha}_m^{(k)}, \boldsymbol{\theta}[i]). \end{aligned}$$

Refining the mixture's parameters is continued if at least one of the following test conditions is fulfilled: a priori weights $|p_k[i] - p_k[i-1]| > \Delta_1$; position characteristics (mean frequency vector) $\|\mathbf{A}_k[i] - \mathbf{A}_k[i-1]\| > \Delta_2$; and scales (covariation matrices) $\|\mathbf{B}_k[i] - \mathbf{B}_k[i-1]\| > \Delta_3$ of spectral classes ($k = 1, 2, \dots, K$). Testing the highest number of iterations $i \leq I_{\max}$ insures against a poor choice of the significance levels Δ_1 , Δ_2 , and Δ_3 of the criteria.

Note that the SWM unsupervised learning algorithm contains two nested cycles. The inner cycle for each spectral class performs the statistical modeling of random frequencies at the S-step and forms estimates (5.6) of the multidimensional integrals in system (5.1) at the W-step. The outer cycle provides the optimization of the spectral model parameters (2.1) at the M-step. It should also be noted that esti-

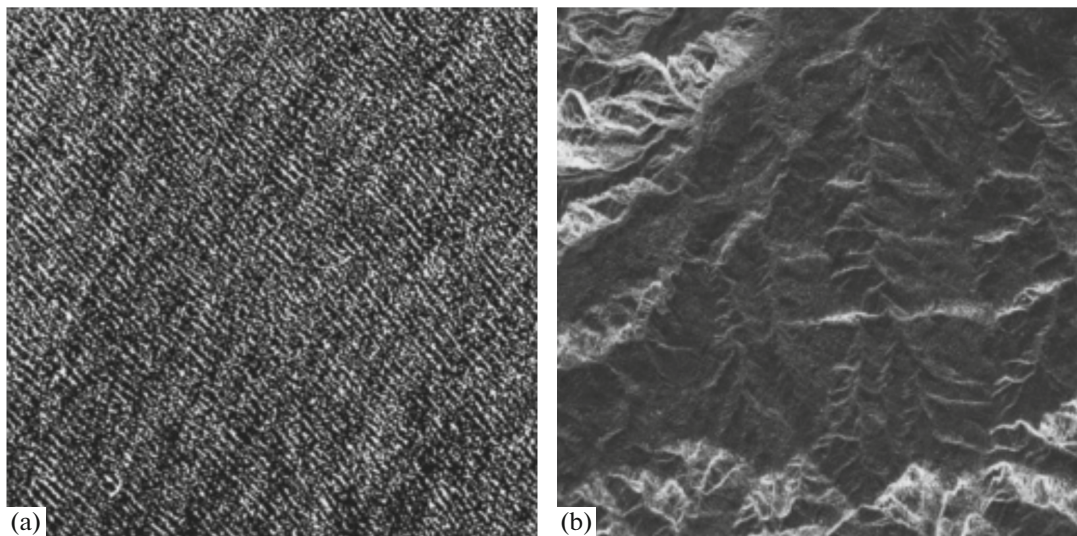


Fig. 5. Satellite radar images: (a) sea surface; (b) mountainous terrain.

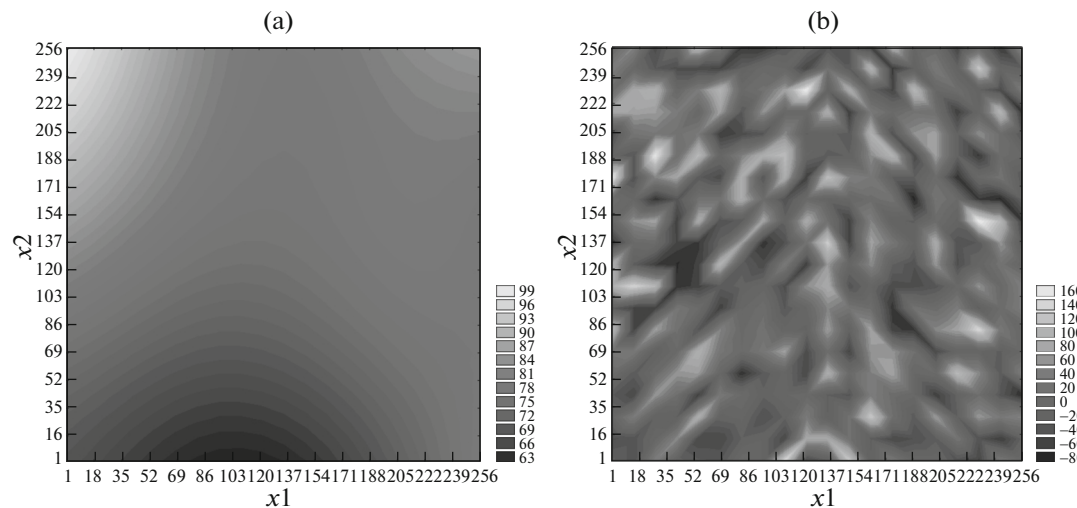


Fig. 6. Structural components of radar image of sea surface: (a) strongly correlated (low-frequency); (b) moderately correlated (high-frequency).

mates (5.6) implement the batch learning mode by the sample of random frequencies. These estimates can be represented in the recurrent form of the successive or combined learning modes of the model [19, 25].

6. COMPUTATIONAL EXPERIMENT

We studied the images obtained as a result of remotely sensing the Earth's surface with satellite synthetic aperture radars. Figures 5a and 5b show the fragments (256×256 pixels) of radar images of the eastern part of the Norwegian Sea [9, p. 71] and mountainous terrain near the city of Muzaffarabad [26] of the Pakistani territory of Azad Jammu and Kashmir acquired by the spacecraft ALMAZ-1 and TerraSAR-X, respectively. The spatial resolution of ALMAZ-1 is $\Delta x_{1,2} = 10\text{--}15$ m; the spatial resolution of TerraSAR-X is $\Delta x_{1,2} = 1\text{--}2.9$ m.

In our opinion, it is rational to study the correlative-spectral properties of the images using the methods of structural data analysis [27], in particular, the multiresolution analysis (MRA) in the basis of a two-dimensional discrete wavelet transform. This methodology allows us to efficiently distinguish the strongly

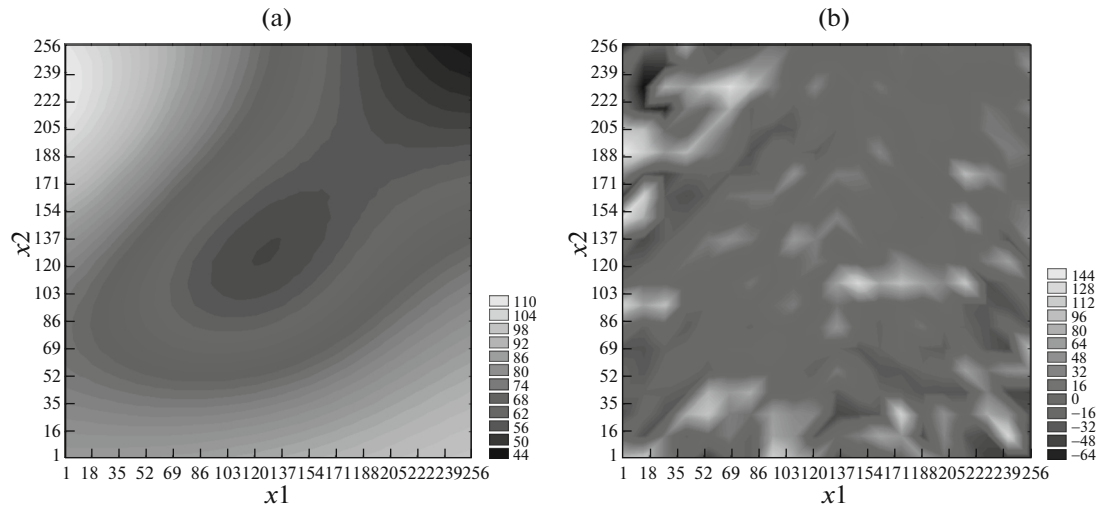


Fig. 7. Structural components of radar image of mountainous terrain: (a) strongly correlated (low-frequency); (b) moderately correlated (high-frequency).

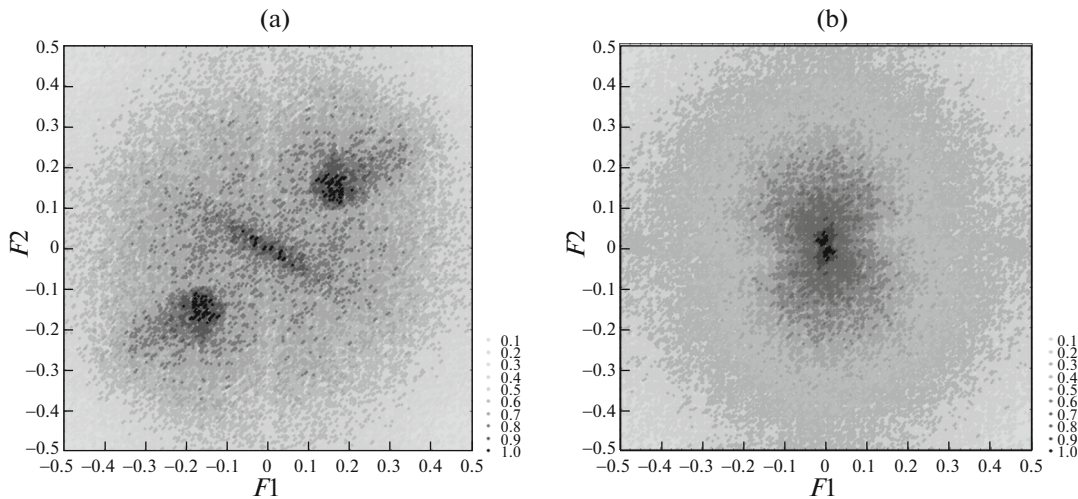


Fig. 8. Cluster structure of two-dimensional sample spectra of high-frequency components of radar images: (a) sea surface; (b) mountainous terrain.

correlated (low-frequency, i.e., trend) and moderately correlated (high-frequency, i.e., quasi-cyclic) components (Figs. 6, 7). In our experiment, we applied the Daubechies wavelets of the 10th degree and nine levels of expansion.

As the trend component of the images of the sea surface, we chose the sum of the ninth detailed component and the approximating component of the MRA (Fig. 6a). The sum of the first to the eighth detail components is taken as an estimate of the quasi-cyclic component (Fig. 6b). The estimate of the trend for the mountainous terrain’s image represents the sum of the eighth and ninth detailed and approximating components (Fig. 7a). The sum of the first to seventh detailed components is taken as an estimate of the quasi-cyclic component (Fig. 7b).

The cluster structure of the two-dimensional Schuster periodogram

$$q_i(F_1, F_2) = \frac{1}{(256\pi)^2} \left| \sum_{n_1=0}^{255} \sum_{n_2=0}^{255} x_i(n_1, n_2) \exp \left\{ -j2\pi \frac{l_1 n_1 + l_2 n_2}{256} \right\} \right|^2, \quad i = 1, 2, \quad (6.1)$$

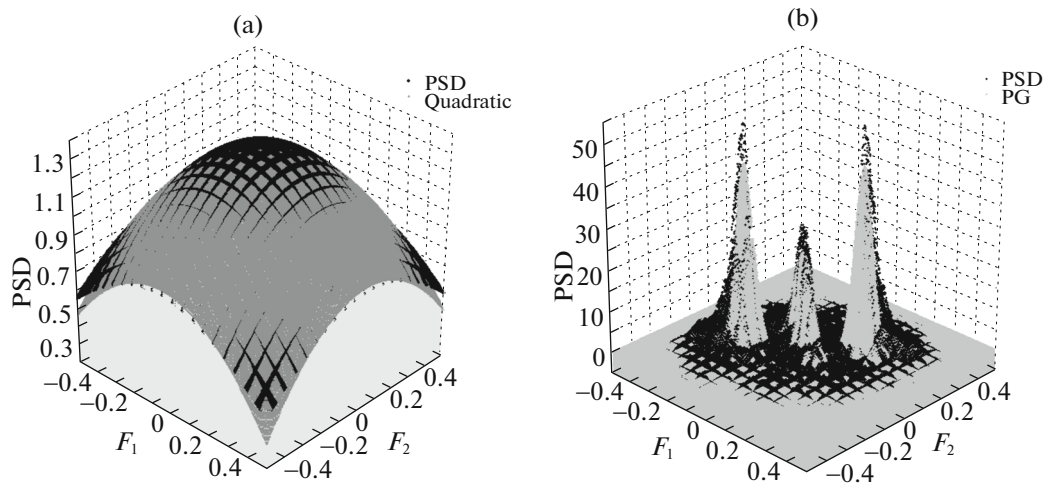


Fig. 9. Structural PSD components of radar image of sea surface: (a) isotropic; (b) anisotropic.

of the quasi-cyclic components $x_i(n_1, n_2)$ of the reference images is demonstrated by the scatter diagrams (Fig. 8) of logarithmic periodograms $\log_{10}\{1 + q_i(F_1, F_2)\}$ converted to the standard range $[0, 1]$ in the coordinates of the normalized spatial frequencies:

$$F_{i,2} = \begin{cases} l_{i,2}/256, & 0 \leq l_{i,2} \leq 127, \\ (l_{i,2} - 256)/256, & 128 \leq l_{i,2} \leq 255, \end{cases} \quad 0 \leq l_{i,2} \leq 255.$$

It is important to note that the classes of a finite mixture (2.1) of generic spectral densities are clearly identified by the structural components of the images; this, in turn, significantly simplifies the procedure of selecting the initial approximations for the parameters of this model. In particular, periodogram (6.1) of the sum of the first to the seventh MRA detailed components, excluding the second, ideally describes the central spectral cluster of the power spectrum of the quasi-cyclic component of the image of the sea surface (Fig. 8). The periodogram of the second detail component describes the side spectral clusters. In other words, the structural decomposition of the radar image of the sea and further spectral analysis of its components allows revealing the main systems and monitoring the parameters of the wind-driven rough water surface.

The classical method of estimating the PSD involves, as is known, the procedures of pseudoaveraging of the Shuster periodogram (6.1). In our experiment, such smoothing procedures consist of two stages. At the first stage, the two-dimensional MRA of the periodograms $q_i(F_1, F_2)$, $i = 1, 2$ of the quasi-cyclic components of the reference images is performed. Here, we also applied the Daubechies wavelets of the 10th degree and nine levels of expansion. As a result of this step, the isotropic PSD components $q_i^{(iso)}(F_1, F_2) = d_i^{(iso)} S_i^{(iso)}(F_1, F_2)$ of the images of the sea (Fig. 9a) and mountainous terrain (Fig. 10a) were distinguished. Here, $d_i^{(iso)}$ are the dispersions of the isotropic PSD components. The sums of the ninth detailed and approximating MRA components were selected as nonparametric estimates of these components. The further analysis has shown that the isotropic PSD components are closely approximated by the two-dimensional polynomials of the second degree (Table 1).

The anisotropic components of the Shuster periodogram (6.1) obviously represent the residuals, i.e., $q_i^{(aniso)}(F_1, F_2) = q_i(F_1, F_2) - q_i^{(iso)}(F_1, F_2)$. At the second stage, the two-dimensional recurrent digital filtering of the residuals with a simple moving average with an 11×11 pixel mask is performed. The results of the

Table 1. Polynomial approximation parameters of isotropic PSD component

Image	$d^{(iso)}$	p_0	b_0	b_1	b_2	b_{12}
Sea surface	276.31	0.3820	1.3018	-1.8111	-1.8111	0.2286
Mountainous terrain	135.45	0.3631	1.3616	-2.1697	-2.1697	0.2487

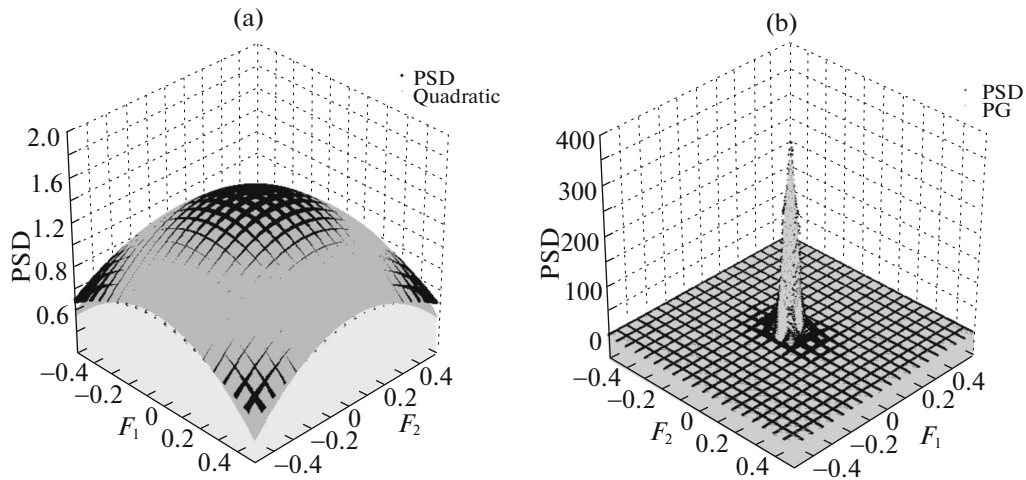


Fig. 10. Structural PSD components of radar image of mountainous terrain: (a) isotropic; (b) anisotropic.

six-fold smoothing by the procedure presented in [28] are chosen as the nonparametric estimates of the anisotropic PSD components $q_i^{(aniso)}(F_1, F_2) = d_i^{(aniso)} S_i^{(aniso)}(F_1, F_2)$ of the sea (Fig. 9b) and mountainous terrain (Fig. 10b). Here, $d_i^{(aniso)}$ are the dispersions of the anisotropic PSD components. The further analysis has shown that the anisotropic PSD components are clearly approximated by the poly-Gaussian (PG) models with the parameters listed in Tables 2 and 3.

As a result, the parametric model of the finite mixture (2.1) of the normalized power spectrum of the images is obtained:

$$S(F_1, F_2) = p_0 S^{(iso)}(F_1, F_2) + S^{(aniso)}(F_1, F_2), \tag{6.2}$$

$$S^{(iso)}(F_1, F_2) = b_0 + b_1 F_1^2 + b_2 F_2^2 + b_{12} F_1 F_2,$$

$$S^{(aniso)}(F_1, F_2) = \frac{1}{2\pi} \sum_{k=1}^3 \frac{p_k}{\sigma_{k,1} \sigma_{k,2} \sqrt{1-r_k^2}} \exp \left\{ -\frac{u_{k,1}^2 - 2r_k u_{k,1} u_{k,2} + u_{k,2}^2}{2(1-r_k^2)} \right\},$$

Table 2. Parameters of poly-Gaussian approximation of anisotropic PSD component of sea surface image: $d^{(aniso)} = 224.85$

k	p_k	$a_{k,1}$	$a_{k,2}$	$\sigma_{k,1}$	$\sigma_{k,2}$	r_k
1	0.1828	0.0	0.0	0.0781	0.0436	-0.8223
2	0.2176	0.1628	0.1392	0.0346	0.0374	-0.0773
3	0.2176	-0.1628	-0.1392	0.0346	0.0374	-0.0773

Table 3. Parameters of poly-Gaussian approximation of anisotropic PSD component of mountainous terrain image: $d^{(aniso)} = 119.31$

k	p_k	$a_{k,1}$	$a_{k,2}$	$\sigma_{k,1}$	$\sigma_{k,2}$	r_k
1	0.0637	0.0	0.0	0.0141	0.011	0.0
2	0.2866	-0.0105	0.0145	0.02	0.0158	0.0
3	0.2866	0.0105	-0.0145	0.02	0.0158	0.0

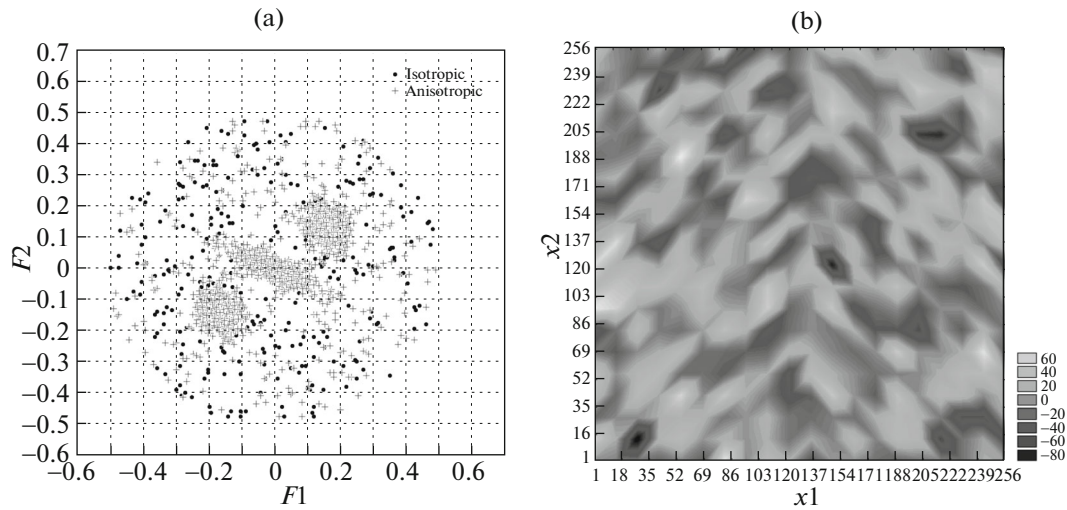


Fig. 11. Statistical modeling results: (a) sample of random frequencies; (b) model images of quasi-cyclic component of sea surface.

$$p_0 = \frac{d^{(iso)}}{d^{(iso)} + d^{(aniso)}}, \quad \sum_{k=1}^3 p_k = \frac{d^{(aniso)}}{d^{(iso)} + d^{(aniso)}}, \quad u_{k,n} = \frac{F_n - a_{k,n}}{\sigma_{k,n}}, \quad n = 1, 2,$$

where the index of the images $i = 1, 2$ is not shown for clarity.

Figure 11a illustrates the scatter diagram of the power spectrum's frequencies of the quasi-cyclic (high-frequency) component of the radar image of the sea surface (Fig. 6b). The statistical modeling of the random frequency vector $\mathbf{\Omega} = (\omega_1, \dots, \omega_N)^T$ was performed using the composition method [2, 12] in accordance with model (6.2) of the finite mixture of standard PSDs. The polynomial isotropic spectral component (Fig. 9a) was simulated by the conventional distributions and reversal methods [2]. The poly-Gaussian anisotropic component (Fig. 9b) was modeled by the composition and correlating transform methods [20, 23]. The radar image of the quasi-cyclic (high-frequency) component of the sea surface that is synthesized using the procedure from Section 5 is illustrated in Fig. 11b.

CONCLUSIONS

We have presented the noncanonical spectral model of multidimensional uniform random fields, whose correlative-spectral properties are adequate to the experimental data. An algorithm that does not require a significant increase in the computational costs with increasing dimensionality of the problem has been developed to identify the parameters of the spectral model. An original procedure has been proposed for the spectral analysis of the images, in particular, the radar images acquired from the remote sensing of the Earth's surface from space. We have obtained parametric models of the power spectrum of the isotropic and anisotropic structural components of the experimental data which ensure the efficient statistical modeling of the images of the underlying surfaces.

REFERENCES

1. L. V. Labunets, *Randomized Spectral Models of Multidimensional Random Fields, The School-Book* (MGU im. N. E. Baumana, Moscow, 2005) [in Russian].
2. A. S. Shalygin and Yu. I. Palagin, *Applied Methods of Statistical Modeling* (Mashinostroenie, Leningrad, 1986) [in Russian].
3. Yu. S. Rasshcheplyaev and V. N. Fandienko, *Synthesis of Random Process Models for the Study of Automatic Control Systems* (Energiya, Moscow, 1981) [in Russian].
4. S. A. Aivazyan, V. M. Bukhshtaber, N. S. Enyukov, and L. D. Meshalkin, *Applied Statistics: Classification and Dimension Reduction, The Handbook* (Finansy Statistika, Moscow, 1989) [in Russian].
5. V. S. Pugachev, *The Theory of Random Functions and its Application to Automatic Control Problems* (Fizmatgiz, Moscow, 1962) [in Russian].

6. G. A. Sergeev and D. A. Yanutsh, *Statistical Methods for the Study of Natural Objects* (Gidrometeoizdat, Leningrad, 1973) [in Russian].
7. A. A. Zagorodnikov, *Radar Shooting of Sea Excitement from Aircraft* (Gidrometeoizdat, Leningrad, 1978) [in Russian].
8. D. A. Yanutsh, *Aerospace Image Decryption* (Nedra, Moscow, 1991) [in Russian].
9. A. V. Dikinis, A. Yu. Ivanov, and L. N. Karlin, *Atlas of Annotated Radar Images of the Sea Surface, Obtained by the Spacecraft ALMAZ-1* (GEOS, Moscow, 1999) [in Russian].
10. V. G. Bondur and V. V. Zamshin, "Space radar monitoring of marine areas in the areas of hydrocarbon production and transportation," in *Aerospace Monitoring of Oil and Gas Facilities*, Ed. by V. G. Bondur (Nauch. Mir, Moscow, 2012) [in Russian].
11. L. V. Labunets, "Parametric modeling of homogeneous random fields measured on a discrete raster," *Elektron. Model.* **13** (3), 10–13 (1991).
12. S. M. Ermakov and G. A. Mikhailov, *The Course of Statistical Modeling* (Nauka, Moscow, 1982) [in Russian].
13. L. V. Labunets and M. P. Mus'yakov, "Parametric model of homogeneous anisotropic random fields," *Izv. Akad. Nauk SSSR, Tekh. Kibern.*, No. 3, 191–199 (1988).
14. M. H. de Groot, *Optimal Statistical Decisions* (McGraw-Hill, New York, 1970).
15. J. T. Tou and R. C. Gonzalez, *Pattern Recognition Principle* (Addison-Wesley, London, 1974).
16. J. Makhoul, "Linear prediction: a tutorial review," *Proc. IEEE* **63**, 561–580 (1975).
17. O. L. Frost, "High-resolution 2D spectral analysis at low SNR," in *Proceedings of the IEEE International Conference on Acoustics, Speech, and Processing, Denver CO, 1980*, Vol. 2, pp. 580–583.
18. L. V. Labunets, "Simulation of a random field using direct and inverse linear prediction," *Elektron. Model.* **11** (6), 98–100 (1989).
19. L. V. Labunets, "Randomization of multidimensional distributions in the Mahalanobis metric," *J. Commun. Technol. Electron.* **45**, 1093 (2000).
20. K. Fukunaga, *Introduction to Statistical Pattern Recognition* (Academic, New York, 1972).
21. I. S. Gradshteyn and I. M. Ryzhik, *Tables of Integrals, Series and Products* (Academic, New York, 2000; Fizmatgiz, Moscow, 1963).
22. L. D. Meshalkin, "Parameterization of multidimensional distributions," *Uch. Zap. Statist.: Prikl. Mnogomer. Stat. Anal.* **33A**, 11–18 (1978).
23. J. M. Geist, "Computer generation of correlated gaussian random variables," *Proc. IEEE* **67**, 188–189 (1979).
24. R. A. Redner and H. F. Walker, "Mixture densities, maximum likelihood and the EM algorithm," *SIAM Rev.* **26**, 195–239 (1984).
25. Ya. Z. Tsypkin, *Fundamentals of the Theory of Learning Systems* (Nauka, Moscow, 1970) [in Russian].
26. www.intelligence-airbusds.com/en/5751-image-detailimg=1779&search=gallery&market=0&world=0&sensor=0&continent=0&keyword=terraSAR%20muzafarabad#.WalAhNSLSt9.
27. L. V. Labunets and V. V. Simakov, "Structural analysis of signals in subsurface radar systems," *Elektromagn. Volny Elektron. Sist.* **18** (8), 49–68 (2013).
28. L. V. Labunets, N. L. Labunets, and M. Yu. Chizhov, "Recurrent statistics of nonstationary time series," *J. Commun. Technol. Electron.* **56**, 1440 (2011).

Translated by M. Chubarova